REPUBLIC OF TÜRKİYE

ALTINBAŞ UNIVERSITY

Institute of Graduate Studies

Electrical and Computer Engineering

BINARY ERROR AND A THREE-LEVEL DIVISION MULTIPLEXING DISPERSION ANALYSIS OF A RAT OPTICAL FIBRE COMMUNICATION SYSTEM

Ali Hussein Oleiwi ALMUKHTAR

Master's Thesis

Supervisor

Asst Prof. Dr. Sefer KURNAZ

Istanbul, 2023

BINARY ERROR AND A THREE-LEVEL DIVISION MULTIPLEXING DISPERSION ANALYSIS OF A RAT OPTICAL FIBRE COMMUNICATION SYSTEM

Ali Hussein Oleiwi ALMUKHTAR

Electrical and Computer Engineering

Master's Thesis

ALTINBAS UNIVERSITY

2023

The thesis titled BINARY ERROR AND A THREE-LEVEL DIVISION MULTIPLEXING DISPERSION ANALYSIS OF A RAT OPTICAL FIBRE COMMUNICATION SYSTEM prepared by Ali Hussein Oleiwi ALMUKHTAR and submitted on 13-4-2023 has been **accepted** for the degree of Master of Science in Electrical and Computer Engineering.

____
Asst. Prof. Dr. Sefer KURNAZ

Supervisor

Thesis Defense Jury Members:

Asst. Prof. Dr. Sefer KURNAZ	Electrical And Computer Engineering, Altinbas University	____________
Asst. Prof. Dr. Abdullahi ABDU IBRAHIM	Electrical And Computer Engineering, Altinbas University	____________
Asst. Prof. Dr. Zeynep ALTAN	Software Engineering, Beykent University	____________

I hereby declare that this thesis meets all format and submission requirements of a Master's thesis.

Submission date of the thesis to the Graduate Education Institute: __/__/___.

I hereby declare that all information/data presented in this graduation project has been obtained in full accordance with academic rules and ethical conduct. I also declare all unoriginal materials and conclusions have been cited in the text and all references mentioned in the Reference List have been cited in the text, and vice versa as required by the abovementioned rules and conduct.

Ali ALMUKHTAR

Signature

DEDICATION

Before anything else, I want to give praise and thanks to Allah Almighty for equipping me with the wisdom, skills, and opportunities to conduct and successfully conclude this research. My deepest gratitude goes out to my parents. They have been the driving force behind everything good that has happened to me, and their love is the fuel that makes it all possible. Finally, I'd want to thank my brother and sister for all of the love and encouragement they've given me during this process.

ACKNOWLEDGEMENTS

I owe a great debt of appreciation to my advisor, Asst Prof. Dr. Sefer Kurnaz, for providing me with the necessary direction, supervision, encouragement, and assistance to complete my study. His willingness to work with me, patience, criticism, and helpful recommendations have been tremendous boosts to my confidence and comprehension. I appreciate his taking the time to check through my work and point out my errors. Finally, I would want to thank everyone who had any part in the creation of this thesis, whether it was via encouragement, prayer, or delivering helpful advice.

Thank you.

ABSTRACT

BINARY ERROR AND A THREE-LEVEL DIVISION MULTIPLEXING DISPERSION ANALYSIS OF A RAT OPTICAL FIBRE COMMUNICATION SYSTEM

ALMUKHTAR, Ali

M. Sc., Electrical and Computer Engineering, Altinbaş University

Supervisor: Asst. Prof. Dr. Sefer KURNAZ

Date: April / 2023

Pages: 44

In this thesis, we analyse the efficacy of the 3LCDM technique in ultra-fast optical fibre networking settings. In comparison to a typical 51 Gb/s non return to zero (NRZ- OOK) system, the dispersion tolerance of a 51 Gb/s 3LCDM system is much larger, as shown by the results. There is an 81 ps/nm chromatic dispersion tolerance at a BER of 10- • 51 Gb/s in the upper tier, and a 98 ps/nm chromatic dispersion tolerance in the bottom tier. Compared to the normal NRZ values for 40 Gb/s, which are about 48 ps/nm, these are much higher values.

Keywords: Fiber Optical, Fiber Bragg Grating (FBG), Inhomogeneous Nonlinear Schrödinger (INLS), Binary Error, Multiplexing Dispersion.

TABLE OF CONTENTS

Pages

LIST OF FIGURES

Pages

ABBREVIATIONS

FBG	:	Fiber Bragg grating
PLC	:	programmable logic controller
IWDM	:	Intensity and Wavelength Division Multiplexing
WDM	:	Wavelength Division Multiplexing
NN	:	Neural Network
PIDS	:	Physical intrusion detection systems
FO	:	Fiber Optic Cable
GTE	:	General Telephone & Electronics

1. INTRODUCTION

1.1 BACKROUND

Recently, fiber optics have surpassed wireless media to become the backbone of telecom and data networks. Multiplexing is often used in optical communication systems to allow several users to share the same bandwidth through a single fiber of the transmission channel. A multi-input system is less expensive than one that uses many fibers for transmission. Multiplexing through wavelength division (WDM) has several uses and is particularly well-suited for implementation in optical fiber communication networks [1]. Another kind of multiplexing used in telecommunications networks is optical code division multiplexing (OCDM). This method assigns a unique code to the data sent by each user, hence allowing for more users to effectively share a single channel [2]. Transmission execution might be worked on over significant distances by giving more thought to multiplexing strategy, scattering the board, and regulation sort. Significant distance optical fiber correspondence frameworks benefit from scattering the board methods since they can fix the contorted signs welcomed on by fiber scattering [3]. Significant distance optical correspondence networks frequently use Frequency Division Multiplexing as a multiplexing method (WDM). Recently, scientists have started analyzing the efficacy of the Three Level Code Division Multiplexing (3LCDM) technique in ultra-fast optical fiber networks. Advantages over Duty Cycle Division Multiplexing (DCDM) [4] exist for supporting many users on a single channel in a WDM system when using the 3LCDM technique with dispersion control. By merging two data streams, which is accomplished with the help of a novel technique called three-level code division multiplexing (3LCDM), the effective bandwidth of wavelength division multiplexing (WDM) is increased by a factor of two. With twice the capacity at half the frequency and a quarter of the bandwidth of RZ and NRZ line coding, 3LCDM is the undeniable winner [5]. As shown in study [1], 3LCDM outperforms the NRZ system in terms of dispersion tolerance, making it a more desirable system overall. It has also come to light that the 3LCDM system, by using WDM, can support a greater number of users. However, research on the viability of transporting 3LCDM data over a WDM system is still in its infancy. Meanwhile, WDM is the most common method of multiplexing data sent across optical fibers. There are losses from dispersion and attenuation when using optical fibers for long-distance transmission [6], [7]. Attenuation may be mitigated by using an optical amplifier [5]. The aim of this research is to examine how well dispersion adjustment works in a 3LCDM over WDM system. A dispersion compensation fiber (DCF) is used to correct the dispersion in an optical fiber [8]. Long-haul transmission systems' distance performance with 3LCDM over WDM will also be examined and monitored.

1.2 PROBLEM STATEMENT

The DCDM technology's encoding method is very similar to that of the 3LCDM approach; However, the 3LCDM technique's decoding procedure has some unique characteristics. 3LCDM can only support two users per channel, whereas DCDM can handle more than two users on a single channel. When comparing their performance with the same number of users (two users per channel), 3LCDM performs better than DCDM in numerous ways. The 3LCDM system makes things simpler by merely employing RZ and NRZ line coding, whereas the DCDM approach adds complexity by employing RZ at varying percentages of duty cycles. Another drawback of DCDM is the requirement for a guard band in the system's clock recovery because it requires more bandwidth than 3LCDM clock recovery.

1.3 OBJECTIVES

Most wireless media have been replaced by fiber optics, making it the major component of telecommunications and data networking infrastructures. Particularly due to the meteoric rise in Internet data traffic, transmission bandwidth utilization has been growing at an exponential rate, creating a massive demand. The following are special qualities of fiber-optic transmission that make it ideal for satisfying this wide bandwidth: Extremely high carrier frequency allows for a tremendous bandwidth. Almost no waste. Easy to carry about and not too bulky to store in a bag. Highly protected and unaffected by electromagnetic radiation from the outside world. This thesis provides a thorough analysis of 3LCDM's performance, contrasting it with that of the more traditional NRZ approach while maintaining the same total bit rate of 40 Gb/s.

1.4 PROJECT SCOPE

Work included in the proposed project scope includes the following:

a. Research on NRZ and RZ coding schemes for the Wide-Distance Multimedia (WDM) system.

b. Examining Opti System’s Library Components (Transmitter Library, Receiver Library, Visualizer, WDM Multiplexer, etc.).
c. Analyzing 3LCDM's Advantages vs WDM.
d. Setup and modelling of a 3LCDM network over a WDM backbone.
e. Analysis of obtained simulation results.

1.5 THESIS OUTLINE

Chapter 1: helps with thesis structure by giving instructions on how to create one. check out the Fiber Bragging' Sensor input, issue description, and scopes while you're at it.

Chapter 2: Includes the Literature Survey.

Chapter 3: Explanation as well as suggesting the method and design of optical fibers, as well as work on the Fiber Bragging Sensor.

Chapter 4: shows the result of the conducted simulation.

Chapter 5: Thesis for conclusion and future work.

2. LITERATURE REVIEW

2.1 LITERATURE REVIEW

Dispersion management in a 3LCDM over WDM system is studied in [9]. The system is tested with a total data rate of 10Gbps across two channels. The highest performance of 3LCDM over WDM is achieved by setting the cut-off frequencies of the Gaussian low pass filter and the Gaussian band pass filter to 18 GHz and 37 GHz, respectively. Finding the optimal received power of the system to achieve BER of 10-9 depends heavily on the input signal. Even at a long-haul transmission distance of 142 kilometres, the 3LCDM over WDM system continues to function well [10]. The effectiveness of three-level code division multiplexing (3LCDM) is measured using a total data rate of 40 Gbps and two different channel counts [11]. The results demonstrate that the suggested 3LCDM method is superior than NRZ-OOK in terms of dispersion tolerance at 40 Gbps. Electrical multiplexing and demultiplexing techniques may use the same wavelength-division multiplexed (WDM) channel [12]. Better dispersion tolerance than the traditional NRZ method means that the WDM channels' capacity may be used to its fullest extent [3]. It is possible to quadruple bandwidth per wavelength using the stated three-level code division approach. Instead of using the wavelength bandwidth, which might lead to interference, code encryption is implemented in the data being sent via many levels [13]. Data rates of 195 Mbps were achieved in the lab, proving the system's viability in local area networks [14]. Non-linear penalties are required for the performance analysis of TDM and WDM signals in 10 Gbps systems [15]. For both long-distance and high-bandwidth communications, TDM signals have a higher quality-of-service (Q) rating than WDM ones. SMFs are suitable for transmitting 10 Gbps of TDM signals when loss and dispersion are correctly adjusted [16]. While using FBGs as dispersion correction devices in SMFs improves performance for both TDM and WDM signals, this is not the case with NZDSFs [17][18]. In practical contexts, the stabilising impact of dispersion control emerges as a result of the interplay of many systems. Specifically, we introduce periodically variable dispersion to NLS ground states in order to create those with crucial non-linearities [19]. To manage the chromatic dispersion (D) of single-mode binary glass fiber cables (T, D), we provide a set of parameters (xc, Anc) for ultra-wide space division multiplexing and ultra-wide wavelength division multiplexing [20]. These parameters can be used to account for any combination of the two variables. A unique mathematical approach is utilised to compute &, Anc in parallel form while maintaining within the actual technical boundaries of 0.0 5 x, 5 0.2, and 0.001 5 Anc 5 0.01 [21]. This creates the necessary compressed dispersion. Overall, linear correlations are discovered, and the current study's basic aspects are included into the 3-D visualisations. The findings of this study have significant implications for the development of high-speed optical communication systems that use optical fibre connections [22][23]. In a 10 Gbps dispersion-controlled system with fibre lengths of 120 kilometres, we explore the use of the RZ and NRZ modulation formats. Both before and post dispersion compensating strategies were used. Both the SMF and DCF input powers are optimised [24]. Using contour plots, we can see that optimal transmission exists. RZ modulation format is superior than NRZ data modulation format once pre and post dispersion correction techniques are optimised [25]. When comparing transmission systems with two, five, ten, and fifteen 120 km fibre spans, the Q factor produced from a RZ transmission system is higher [26][27]. The DCDM method's underlying concept and the empirical evidence supporting it are explored. Multiple users' data, differentiated by their own duty cycles, is sent across a single optical wavelength [28]. More than two users may share a single WDM channel by using the multiplexing/de-multiplexing of electrical signals [29]. This results in greater channel capacity utilisation at a single-user clock rate, reduced spectrum bandwidth, and enhanced dispersion tolerance. By way of illustration, a DCDM system with multiplexed three users is shown to function successfully when tested at up to 40 Gbps per user speed, providing a maximum throughput of 120 Gbps per WDM channel [30]. In order to do simulations, [31] a RZ pulse generator is used. Different RZ pulses and their quality factors are shown in this study. If we assume that Gaussian pulses, which perform better than others, are responsible for these improvements, we may infer that increasing the laser's power also improves the outcomes. Increasing the laser power to 2 dbm improves the quality factor [32]. It has been noticed that the strength of the laser is a crucial factor in the simulation process. Quality factors of 5 or more are rated excellent by the Open Film Certification (OFC). At a data rate of 40 Gbps and a connection length of 360 km, this simulation study achieves a quality factor of 11.84. [33]. Three different symmetric dispersion correction systems are used to examine the impact of SPM on the performance of 40 Gbps ODCDM over a distance of 400 kilometres [34]. Based on the data, it seems that using a hybrid compensation technique that takes use of both pre and post dispersion is the most effective method for this setup [35]. Our findings indicate that ODCDM may be employed in MAN and WAN applications with little degradation from the SPM effect for error-free communication if a proper dispersion correction technique with optimal parameters is used [36].

2.2 OPTICAL FIBER

A fibre optic is a translucent, malleable strand of silica or plastic that may be adjusted to a width slightly wider than a human hair. Light fibres are widely employed in fibre optic communication because they allow for longer distance transmission and better data speeds than electrical connections [37].

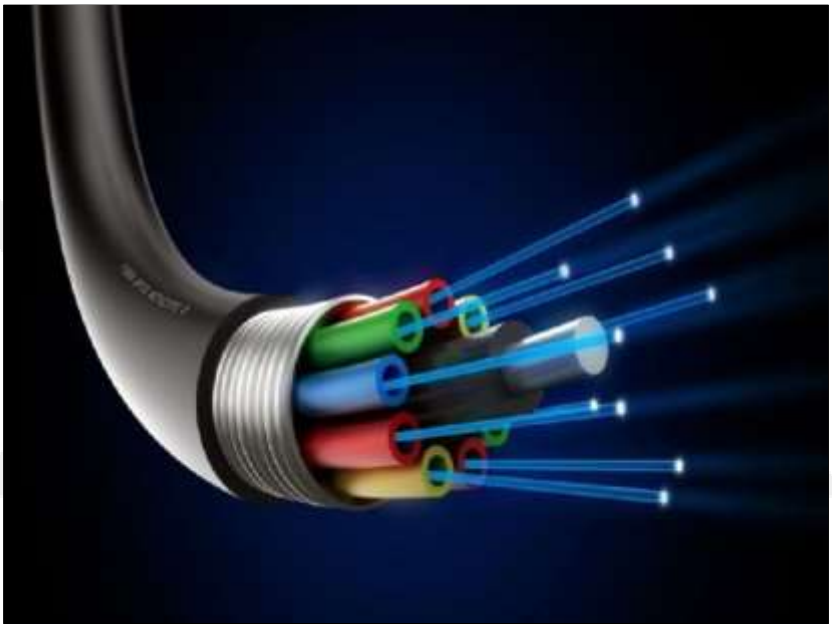

Figure 2.1: Optical Fibber [38].

2.3 IMPAIRMENTS TO FIBER-OPTIC COMMUNICATION SYSTEMS

Linear and nonlinear effects may be distinguished as causes of signal degradation in optical fibre transmission. These consequences in optical fibre networks are briefly discussed here.

2.3.1 Limitations in a Linear Fashion

The linear impairments in optical fibre are described by the Linear Schrödinger Equation (LSE), where the propagation constant () is first extended into a Taylor series around the carrier frequency; here, the series expansion includes just the first three components. The LSE may be calculated using the following formula if the above is true: [39].

$$\frac{\partial \boldsymbol{A}}{\partial z} + \frac{\alpha}{2} A + \beta_1 \frac{\partial \boldsymbol{A}}{\partial t} + \frac{j}{2} \beta_2 \frac{\partial^2 \boldsymbol{A}}{\partial t^2} - \frac{1}{6} \beta_3 \frac{\partial^3 \boldsymbol{A}}{\partial t^3} = 0 \tag{2.1}$$

where A is the amplitude of the optical field, is the attenuation coefficient, 1 is related to the group velocity, 2 is the group velocity dispersion that causes pulse widening, and 3 is the third-order dispersion parameter.

2.3.1.1 Attenuation in fibbers

As the light travels through the optical cable, some of its energy is lost. Light absorption by the material, Rayleigh linear scattering, and Mie linear scattering are the primary causes of power loss [40]. Optical power decreases as its length along a lossy fibre increases in the z direction, according to Beer's law, which may be expressed as:

$$P(z) = P\,(0)\exp(-\alpha z) \tag{2.2}$$

power launched into the fibre, denoted by P (0).

At 1550 nm, it is stated that the attenuation coefficient of optical fibres is just 0.17 dB/km. In Figure (2.2), we see the whole range of losses in a fused silica fibre from a variety of different causes [41]. Near 1550 nm, this fibber’s loss value is at its lowest. Larger losses. are seen at shorter wavelengths, with values exceeding a few dB/km in the visible spectrum [42].

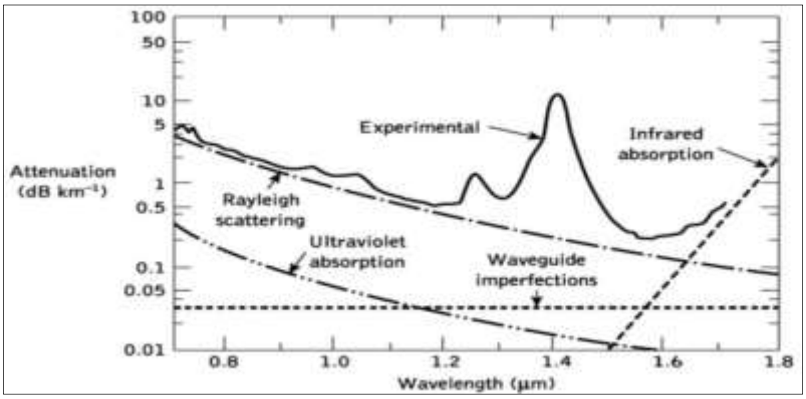

Figure 2.2: Comparison of the Measured Loss Spectrum of a Single-Mode Silica Fibre [43]

2.3.1.2 Differentiation of colours

The amount of information that can be sent and how far it can go across a fibre connection is limited not only by attenuation, but also by dispersion. According to Eqn. (2.3), 1 determines how quickly the optical pulse envelope travels through the fibre [44].

$$\beta_1 = \frac{1}{v_G} = \frac{1}{c}(n + \omega \frac{dn}{d\omega}) \tag{2.3}$$

the optical frequency, the speed of light in a vacuum c, and the linear refractive index n. Broadening of optical pulses during propagation is often attributed to Group Velocity Dispersion (GVD). The GVD parameter, 2, in Eqn. (2.3) is defined by [45].

$$\beta_2 = \frac{1}{c}(2\frac{dn}{d\omega} + \omega\frac{d^2n}{d\omega^2}) \tag{2.4}$$

Taking the first derivative of 1 with respect to wavelength yields the dispersion parameter.

$$D = \frac{d\beta_1}{d\lambda} = -\frac{2\pi c}{\lambda^2}\beta_2 \approx \frac{\lambda}{c}\cdot\frac{d^2n}{d\lambda^2} \tag{2.5}$$

Let's go back to the equation (2.6) As before, the GVD slope parameter is thought to be 3 = d2d, which is related to the dispersion slope parameter [46].

$$S = \frac{d\beta_2}{d\lambda} = -\frac{4\pi c^2}{\lambda^3}\beta_2 + (\frac{2\pi c}{\lambda^2})^2\beta_3 \tag{2.6}$$

Within the area of 2 = 0, when dispersion is at a minimum, the GVD slope becomes the primary factor in determining how much energy is transmitted [47].

To get rid of 1 from Eqn, we create a delayed time frame T = t zvG that travels with the signal at the group velocity (1.1). Furthermore, the impact of the GVD slope may be disregarded when Standard Single-Mode Fibbers (SSMFs) or other varieties with suitably high GVD are used. For these input values, we have [41] as the solution to Eqn. (2.7) [48].

$$\frac{\partial \boldsymbol{A}}{\partial z} + \frac{\alpha}{2}\boldsymbol{A} + \frac{j}{2}\beta_2\frac{\partial^2 \boldsymbol{A}}{\partial t^2} = 0 \tag{2.7}$$

The dispersion profile in silica SSMF is a function of both the dispersion of the waveguide and the dispersion of the material [49]. The profile of dispersion seen in Fig. is the result of the addition of these two factors (1.2). The wavelength at which dispersion is zero is 1324 nm, while the wavelength at which D = 16 ps/km/nm is 1550 nm. Because of how fused silica is made, the material's dispersion is fixed [50]. However, the dispersion of the waveguide is governed by the fibber's effective refractive index. Fibbers with varying degrees of dispersion may be produced by altering the index profile, allowing for the creation of anything from a Dispersion Compensating Fibber (DCF) with D = 80 ps/km/nm to a non-zero dispersion shifting fibre with D = 4 ps/km/nm. [51].

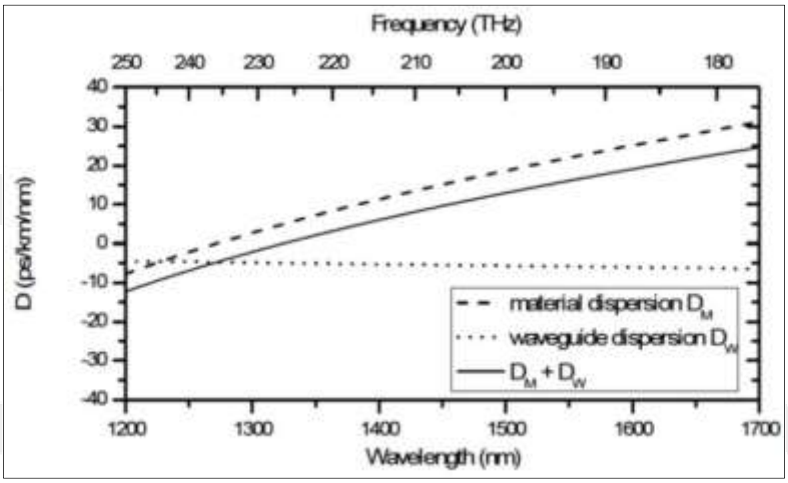

Figure 2.3: The Wavelength and Frequency Dependence of the Dispersion Characteristic of a Typical Standard Single Mode Fibre [52].

2.3.1.3 Dispersion of polarization modes

Polarization of light is a feature of electromagnetic waves that characterises the orientation of transverse electric field fluctuations [53]. There are two distinct polarisation states, x and y, in SSMF. Representing Stokes parameters, which may be simply defined using a Poincare sphere, allows one to explain the polarisation of light [54]. Figure 2.3 illustrates the SOP by depicting the Poincare sphere, which consists of four stocks parameters in terms of optical power. Dual-polarization transmission is possible with an SSMF [55]. These polarisation states are orthogonal to one another. Variations in temperature and fibre birefringence owing to mechanical stress may alter the modes' orthogonality, though [56][57].

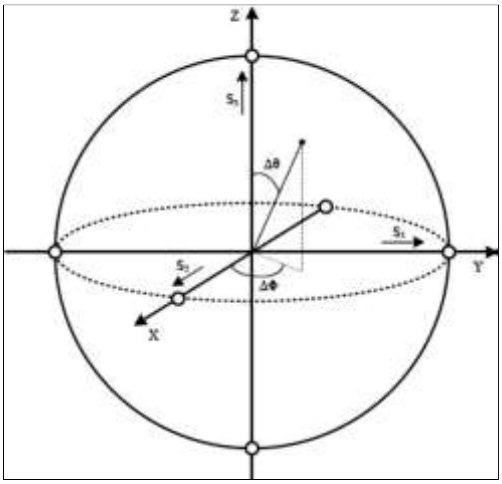

Figure 2 4 : Round Like in Poincare. These Stocks Factors are S1, S2, And S3. Using the Formula S2 = S2 + S2 + S2, We May Get The Fourth Parameter, S4 [58].

It is common for the SOP to shift as the fibre length approaches or exceeds a few kilometres. In mathematics, modal birefringence, Bm, is defined as [59].

$$B_m = \frac{|\beta_x - \beta_y|}{2\pi} = |n_x - n_y| \tag{2.8}$$

where x and y are the respective propagation constants and nx and ny are the effective refractive indices of the two modes [60]. The axis with the highest group velocity is typically referred to as the "fast axis," while the axis with the lowest group velocity is referred to as the "slow axis." A pulse with a linear polarization is shown to travel through a fiber at an incidence angle of 45 degrees (4 rad) from the slow axis in the figure (2.4) [61]. Two orthogonal modes, one in the slow axis and one in the fast axis, both of equal strength, are simultaneously excited by the optical pulse in this case [62]. The receiver receives two pulses because the energy randomly divides between the two polarization states as it travels down the fiber [63]. The time delay between the two pulses is the

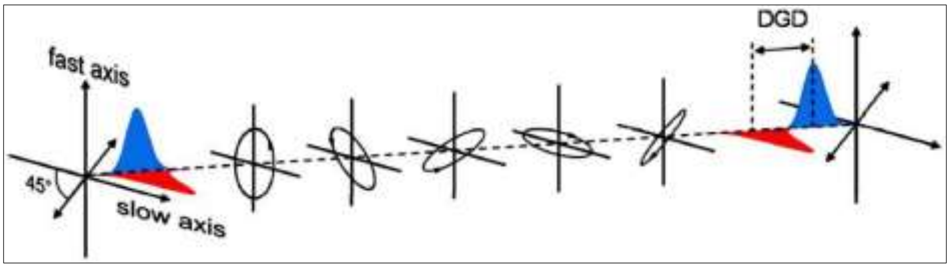

Figure 2.5: Fiber Length Squared.

differential group delay (DGD) T, which has a Maxwellian distribution around its mean. Mean DGD rises proportionally to the fiber's Polarization Mode Dispersion (PMD) parameter, which typically ranges from 0.01 to 0.5 ps/km [64], and with fiber length squared [65].

2.4 A SYSTEM OF FIBER OPTIC CONNECTIONS

Customers final Internet connection is made possible via access networks. Different access technologies, such as copper, wireless (air), and optical fibre, are grouped together based on the medium through which data is sent [66]. For connection, a fibre access network is superior to others due to the use of optical fibre, which allows for more capacity and greater range [67]. At most cases, an optical line terminal (OLT) is installed in the central office (CO) and optical network units (ONUs) are installed at the end points through fibres [68].

2.4.1 Optical Passive Networks

In order to link numerous fibers together, passive optical networks (PONs) rely solely on passive plant components like wavelength or power splitters and combiners [69]. When compared to active optical networks, which necessitate active equipment in the field, these network topologies improve reliability while also lowering costs and energy consumption [70]. Numerous distinct PON architectures can be realized using multiplexing techniques, including but not limited to:

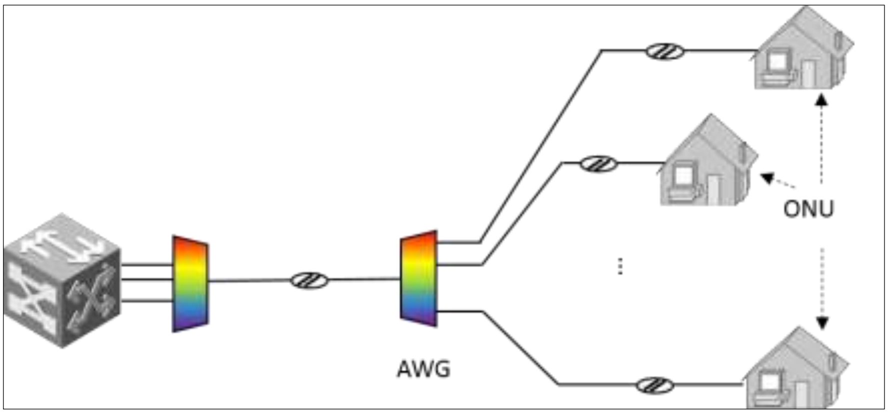

Figure 2.6: Conventional Design for a WDM-PON Network [71].

Multiple PON technologies, including TDM and WDM, are put to use. Gigabit Capable PON (GPON) and Ethernet PON (EPON) are two examples of widely used 1.1 Gb/s TDM-PONs [28] and [72]. 10 Gb/s TDM-PON deployment, such as XG-PON1 [30] and 10G-EPON [31], is just beginning. Each ONU is given a time slot in which to receive packets sent downstream from the OLT through optical splitters [73]. When the OLT serves a large number of ONUs, the signals experience considerable insertion loss due to the power splitters. It restricts the available power in the connection and therefore its range. Since all of the ONUs must share the bandwidth provided by a single wavelength in the future, it will be challenging to meet the customers' expected bandwidth needs [74].

Several wavelength channels are multiplexed and distributed to individual ONUs; therefore, the moniker "WDM PON." As one of the most effective strategies for increasing PON capacity, it is receiving a lot of attention. WDM PON was initially used in 2007 in Korea [75]. Typical WDM-PON architecture is shown in Figure 2.6 Commonplace design for a WDM-PON network. In TDM-PON, the optical power splitters are substituted by wavelength de- multiplexers like AWGs. WDM-PON enables each subscriber to have one or more dedicated wavelengths, while with TDM-PON all 32, 64, or more ONUs must share a single wavelength [76]. With this capability, you can easily adjust to meet the bandwidth needs of a wide variety of consumers. Moreover, with WDM-PON, the power budget issue may be resolved by using an AWG at the distant node, which has significantly lower insertion loss than a power splitter. As a result, a WDM-PON can cover a much more ground than a TDM-PON [77].

One easy way to increase access capacity in WDM- PON and provide service to more customers is to decrease the wavelength spacing and increase the number of channels. Differences between neighbouring wavelengths in DWDM-PON are less than 100 GHz [78]. However, while transmitting high-bandwidth signals, the system becomes more vulnerable to crosstalk due to the narrow channel difference. Transmission performance may be severely impacted by the laser source's wavelength drift.

An OFC is a possibility for the multi-carrier source in a DWDM-PON system because it can produce numerous carrier frequencies from a single wavelength at constant amplitude and spacing. Mode-locked lasers [79], supercontinuum optical sources [80], and the nonlinear effects of optical fibres [81] are all part of the standard OFC generating method. However, mode-locked lasers may be challenging to manage. Methods based on a supercontinuum source are notoriously difficult to construct. Methods based on the nonlinear effect are costly because they need the use of very long lengths of highly nonlinear fibre. In addition, nonlinearity-based OFC creation requires a large amount of optical input power. The use of Mach-Zehnder modulators (MZMs) in OFC production has recently become more appealing due to the discovery of an electro-optic modulator based on a LiNbO3 crystal waveguide [82]. In these methods, the channel spacing between any two adjacent tones is fixed with respect to the steady underlying radio frequency (RF). While [83], suggests using specialised driving RF, [84], suggests using specially designed high dispersion medium to create OFC. Each one is really costly.

2.4.2 Radio Over Fibre Optics Systems

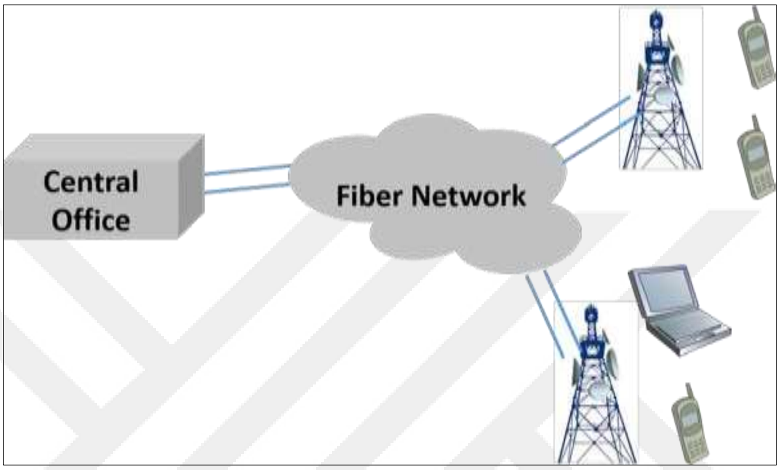

Figure 2.7: A RoF Communication System's Fundamental Diagram.

The goal is to create a global network in which any two points in the globe may instantly establish a connection with any other. However, the quality of a wireless signal decreases dramatically as the distance from which it is sent grows. For this reason, it is extensively used for backhaul, or the transmission of radio frequency (RF) signals between a central office (CO) and a set of cell sites.

The RoF connection differs from a regular digital baseband optical link [85], for transferring RF signals, as seen in Figure 2.7 Typically, an electrical-to-optical (E/O) converter is used to transform the baseband signal into the optical spectrum before it is sent through a fibre optic cable. Before amplifying and transmitting the signal into the air, the base station (BS) performs signal processing, such as demodulation and modulation of the baseband signal. There is an RF up-conversion module and an E/O conversion module in the RoF system, respectively, that transform the wireless signal into an optical one. Since baseband signal processing is no longer required at the cell site, the RoF approach makes cell site setup easier [86].

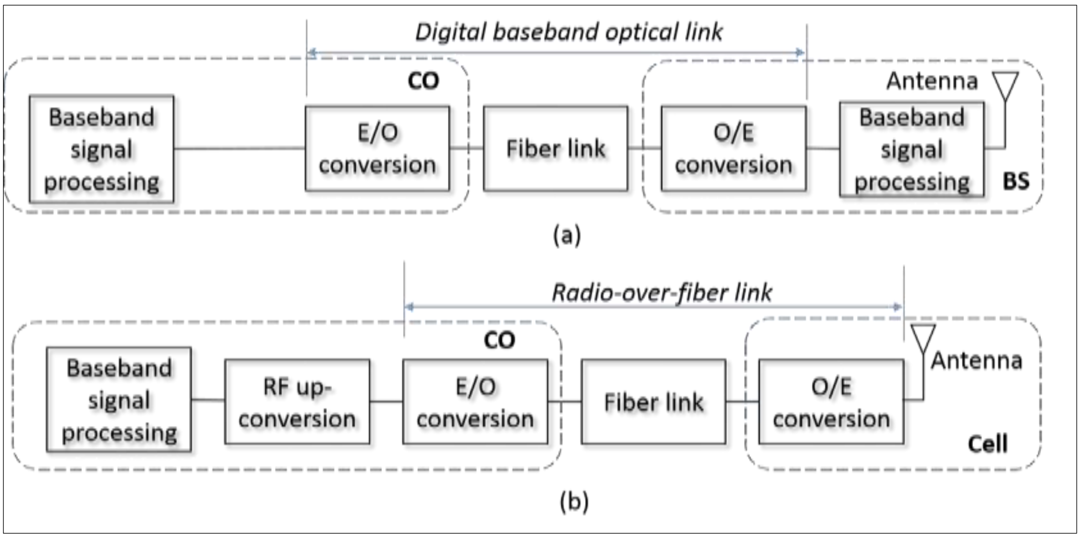

Figure 2.8: (a) A Digital Baseband Optical Connection and (b) Radio Over Fibre (Rof) Transmission Diagram.

Due to the increasing need for bandwidth in wireless communication, the millimetre wave (MMW) band is attractive. The MMW band, which has a waveband of 1 to 10 millimetres and ranges from 30 to 300 gigahertz, has the potential to offer a significant amount of capacity for wireless connectivity. For instance, standards have been established for short-range wireless applications in the 60 GHz band [87], and interest in frequencies above 100 GHz is growing [88]. However, in comparison to the operating bands that are currently utilized by mobile service providers, the MMW band has greater propagation attenuation from the surrounding environment. As a result, the typical transmission distance for MMW is less than 100 meters. In light of this, it becomes more appealing to use RoF technology to send the MMW signal to the antennas [41].

MMW-based RoF systems have been the focus of numerous studies. It is possible to generate multi-band MMW signals from an optical LO by employing a single Mach-Zehnder modulator (MZM) in the cyclic predistortion (CS) and heterodyne mixing processes, as described in [17]. The paper's recommendation for creating a multi-band signal with a dual-drive modulator and two distinct clock signals necessitates the use of a high frequency synthesiser. Another way to make multi-band MMW is to use an optical frequency comb (OFC) with a flat spectrum and uniform frequency spacing [18]. Several other MMW bands are generated by beating the other comb lines while one is used for downstream data transfer. It should be noted, however, that the vast majority of existing approaches, such as [17][19], modify several MMW bands using the same data, which is inefficient.

2.5 NETWORKS INSIDE DATA CENTERS

The significance of datacentres continues to grow in the modern day. Our civilization would not be as efficient or productive without the datacentres that host our social media, email, web searching, and online consumer services. As previously noted, data-intensive applications pose a significant difficulty in terms of power usage. Optical.

Table 2.1: Future Computer Systems Must Balance Performance, Bandwidth Needs, and Power Consumption [42, 43].

ear	**Maximu m Performance**	**Broadban d standards**	**Consumption of power restricted**
013	11 PF	1 .5 PB/s	6 MW
017	101 PF	2 1 PB/s	1 1 MW
021	1001 PF	4 01 PB/s	2 1 MW

* PF: Peta operations with floating points per second

Communication's high capacity, low loss, and great energy efficiency are crucial to developing a sustainable networking option for data centres. For this reason, this thesis places a premium on researching solutions to the issue of energy consumption in datacentre networks (DCNs), which are the networks used inside datacentres.

2.5.1 Datacentre Energy Use

Table 1 details the expected future datacentre systems' computing power, bandwidth needs, and energy usage. However, the pace of rise of power consumption can only be two [42][43], times every four years, whereas the predicted peak performance and bandwidth requirement of datacentres is expected to climb fast. The first step in solving the datacentres power consumption issue is identifying its root cause. Figure 2.9 from [41], depicts the breakdown of IT energy use in a mega datacentre, with the network accounting for around 30% and servers and storage using the remaining 70%. Half of the networking niches are occupied by access switches at the top-of-rack (ToR).

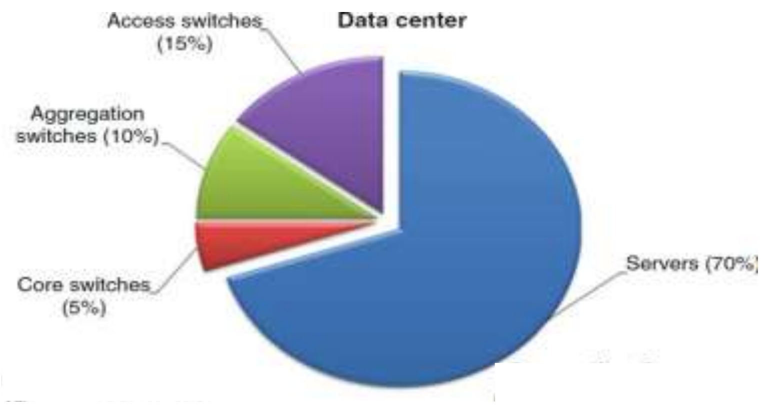

Figure 2.9: Methods for Balancing a Datacentre's Energy Usage [44].

the whole switching capacity, etc. Therefore, it is crucial in the design of energy-efficient DCNs to greatly minimise the power spent at ToR.

2.5.2 Datacentre Traffic Characteristics

To effectively build a DCN, it is essential to have a firm grasp on the primary characteristics of the server traffic that will be produced. Various types of traffic have different characteristics, yet they also have certain commonalities, as we'll see below.

a. Datacentre traffic flow localization refers to how much of the data centre's traffic is kept inside the facility. Traffic between servers in the same rack is called intra-rack traffic, whereas traffic across racks is called inter-rack traffic. Different datacentres see varying amounts of each sort of traffic. In cloud computing datacentres, the ToR switches handle up to 80% of the intra-rack traffic. The high volume of intra-rack connections in these datacentres makes it imperative to cut down on edge-tier power consumption in order to solve the thermal dissipation issue of DCNs.
b. The majority of data sent between servers is relatively short in length (lasting less than a few hundred milliseconds) and bandwidth (in size). The intra-datacentre connectivity must have a minimal reconfiguration overhead to guarantee a short latency of the traffic.
c. It's common for intra-rack traffic to be quite burst, but traffic in the aggregation and core tiers is often less so. Due to this characteristic, the design of DCNs' several layers must accommodate a wide range of conditions.
d. The typical number of concurrent flows per server is roughly 10 in most data centres [23]. Multi-cast support should be considered during DCN architecture design.

2.5.3 Datacentre Network Topologies that Use Less Energy

Since existing datacentre commodity Ethernet switches may not be able to handle the anticipated traffic surge with acceptable energy usage [45], there is a pressing demand for alternatives that are both high capacity and energy efficient. DCNs may benefit greatly from optical transmission technology because to its high throughput, low latency, and low power requirements [44]. Communication between servers, racks, and clusters is managed through switches at various layers. Many different optical switching-based interconnects for DCNs have been studied in the last few years. There have been suggestions for hybrid optical/electronic solutions to the problem of increasing capacity while decreasing power consumption; examples are HELIOS [46], and C-through [47]. These strategies use optical switching for managing massive flows, but they also retain electrical switches for handling traffic at the packet level. Researchers have also looked at all-optical interconnect topologies for the aggregation or core layer [48][50]. Optical packet switching is used to provide fine-grained switching in [48], however it calls for O/E and E/O conversions at every stage of the buffering process. The optical interconnects based on microelectromechanical systems (MEMS) suggested in [49] are inefficient for burst traffic patterns and need significant time to configure connections. To facilitate high-throughput DCNs, a hybrid SDM/TDM network is proposed in [50]. However, multi-element fibre (MEF) is prohibitively expensive, thus it cannot be used to link racks. Additionally, an SDM-to-WDM converter is required for the approach in order to execute the connection between two racks in different datacentres via the metro network, but such a device is not currently commercially available.

Cutting down on the number of electrical components used is one technique to save power in a datacentre. Optical switching is the foundation of several already-existing DCN designs [48][50]. In these architectures, electrical switches in the aggregation and core layers are often replaced with optical ones. Incorporating optical switching at the data centre’s upper tiers can save some power, but only so much [25]. However, because of the many racks in a datacentre, ToR switches may account for as much as 90 percent of the facility's total switching energy consumption [51]. As a result, enhancing datacentre efficiency necessitates prioritising the reduction of ToR switching energy usage. Passive optical interconnect (POI) is the subject of some literature at the threshold of recognition (ToR) [24][52]. When compared to switch-based systems, passive components like optical couplers have inherent advantages in terms of cost, energy consumption, and dependability. Furthermore, since no hardware reconfiguration is required, the POI designs have the potential to have high latency performance. In [52], the scalability of a coupler-based POI is evaluated solely in terms of the insertion loss, which is necessary but not sufficient. A wide range of physical layer variables should be taken into account during the scalability assessment. The receiver type, operating bandwidth, modulation formats, and decision algorithms are just a few examples.

2.5.4 Intra-Datacentre Optical Connections with Advanced Modulation Formats

DCN is very cognizant of the price and energy usage of transceivers because of the vast number of transponders it uses. In DCNs, short-range communications using intensity modulation and direct detection (IM/DD) methods are common due to their ease of implementation and lower cost compared to coherent alternatives. The bit rate per wavelength in IM/DD techniques is calculated by multiplying the symbol rate in bits per second (Baud rate) by the symbol size in bits (modulation order). On-off-keying (OOK) intensity modulation is the simplest form of IM/DD. However, a high data rate necessitates the use of electro-optical components with a wide bandwidth. Increasing the modulation order, or using a more complex modulation structure, is one technique to do this. As a result, M-PAM (54–57) and DMT (58–59) over low-cost and low-energy integrated transceivers have emerged as Datacom's two mainstays.
For instance, 4-PAM and 8-PAM both refer to modulations with 4 amplitude levels, while M-PAM stands for multi-level intensity modulation [59]. Transmissions using M-PAM have a spectral efficiency that is log M times better than those using binary modulation (like OOK) at the same data rate.

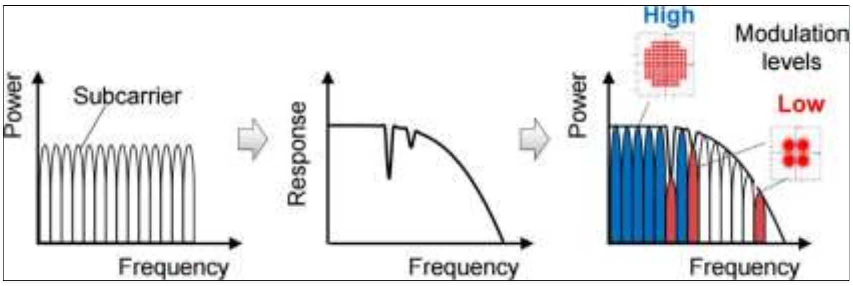

Figure 2.10: The Subcarriers' Power and Bit Allocation Based on the Channel Response. [63].

DMT is a type of OFDM that uses a different set of carriers than OFDM because it is a multi-carrier technology. Figure 8 depicts how DMT divides the spectrum, with each subcarrier using a small portion of the channel capacity. The channel response at the frequency of each subcarrier is used to calculate the allocation of bits and power for that subcarrier. To put it another way, DMT maximizes the utilization of the spectrum by assigning lower-order modulation formats to subcarriers with lower SNRs and higher-order modulation formats to subcarriers with higher SNRs.

Table 2.2 provides a summary of the literature [60]-[64] comparing M-PAM with DMT in terms of energy usage, performance, etc. While DMT provides clear benefits in spectrum use and resilience in the face of non-flat channel response, M-PAM has lesser implementation complexity and lower power consumption.

Table 2.2: M-PAM and DMT: A Comparison [60–64].

	***M*-PAM**	**DMT**
Complexity of the implementation	+	O
Use of power	++	+
Utilizing the spectrum	+	++
Robustness	O	++

Which is meaning ++ very good, + good and O medium

2.6 BASIC STRUCTURE FOR FIBER-OPTIC

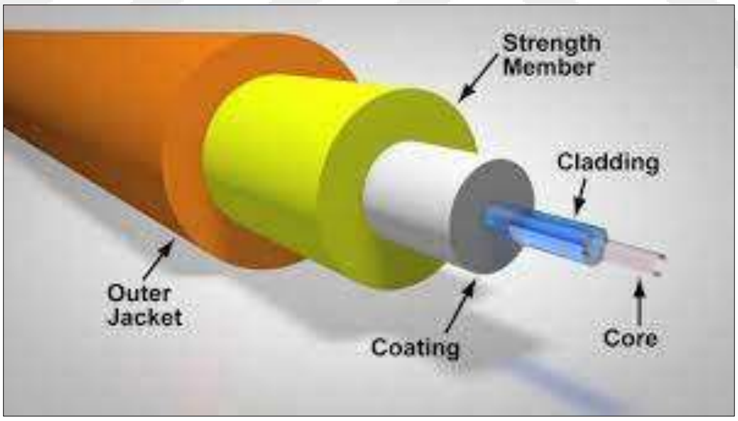

Figure 2.11: The optical Basic Structure [37].

Figure 2.11 depicts the fundamental make-up of an optical fibre. Optical fibers commonly incorporate:

a. An innermost core layer: The optical fiber's glass core is the first layer within the cable. The light penetrates all the way to the centre.
b. Cladding Layer: The cladding layer protects the glass core. As with the core, this layer is composed of glass, but its refractive index is lower. The cladding layer is either thicker or thinner depending on the wavelength that will be sent along the fibre.

c. Protective Jacket Layer: The protective jacket layer serves as the outermost layer. The optical cable is reinforced here to withstand mechanical stress. When more reinforcement is needed, a Kevlar coating is sometimes applied.

Transparent cladding with reduced refraction index around a core [38][39]. Because of absolute internal reflection, the fibre essentially functions as a waveguide, focusing light at its centre. Multi-mode fibres provide many engendering routes, also known as transverse modes, whereas single-mode fibres support just one (SMF). Most often used for short-distance correspondence connects and applications requiring strong force transmission, multi-mode fibres have larger core sizes [40]. The majority of communication links over a thousand metres in length use single-mode fibres (3,300 ft).

2.7 MANUFACTURING MATERIAL

Glass optical fibres are often made from silica [41], but for longer-frequency infrared or other uses, additional materials such as fluor zirconate, fluor aluminate, glasses made of chalcogenides and crystalline crystals like sapphire are both put to use. There are certain materials, such the chalcogenides, that may increase the refractive index of glasses formed from silica and fluoride to as high as 3. On average, there is a 1% difference between the centre and cladding indices.

2.7.1 Silica

Across a broad range of frequencies, silica exhibits exceptional optical transmission. Silica may have exceptionally poor retention and dissipation capabilities of the desired 0.2 dB/km in the near-infrared (close to IR) part of the spectrum, namely about 2.6 m. In order to construct integrated circuits and discrete transistors, ultra-pure silicon is essential. This makes it feasible to achieve such shockingly low losses. Transparency in the 1.4-m range is enhanced by keeping the proportion of hydroxyl groups low (OH). Transmission in the UV spectrum, however, is improved by a larger OH concentration.

2.7.2 Glazed with Fluoride

Glasses of high optical quality may be created from fluorides of various metals, and this group is known as "fluoride glass." Due of their thinness, preventing crystallisation while manipulating it through the glass transition is a challenging task (or drawing the fibre from the liquefy).

Heavy metal fluoride glasses, on the other hand, have incredibly low optical attenuation but are difficult to produce, extremely fragile, and poorly protected against dampness and other environmental impacts. Their finest quality is that unlike other oxide-based glasses, they lack the hydroxyl (OH) absorption band (3,600-2,500 cm1; i.e., 3,877-3,125 nm or 2.78-3.13 m).

2.7.3 Phosphate-Based Glass

Different metal metaphosphates are used to create the optical glasses that make up the phosphate glass family. At least four distinct structures exist for phosphorus pentoxide (P_2O_5), serves as the structure hinder for this glass, rather than the SiO_4 tetrahedra seen in silicate glasses. P_4O_{10} atoms make up the most recognised polymorph.

3. METHODOLOGY

3.1 INTRODUCTION

This section introduces the concepts of forward engendering of signs obtained from forward spread transmission boundaries, which are then used to illustrate the nonlinear Schrödinger condition (NLSE). To reconstruct the original sent signal from the distorted got signal, one may invert the nonlinear Schrödinger equation (NLSE). A mathematical model that includes the negative sign with the primary dispersal coefficients, such as the scattering D and the nonlinear coefficient, is used to deal with this.

3.2 TLCDM OVER WDM THEORY

3.2.1 WDM

The optical fibre multiplexing industry has settled on the wavelength division multiplexing (WDM) technology as the gold standard. It is well knowledge that dispersion and attenuation cause losses when using optical fibres for long-distance communication. The use of an optical amplifier is the answer to the problem of attenuation loss. Dispersion compensation fibre (DCF) is used to correct for dispersion in optical fibre.

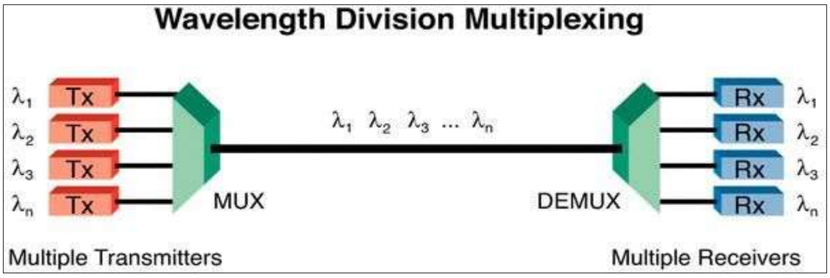

Figure 3.1: Multiplexing on a Wavelength Scale.

Transmission performance may be improved over long distances by giving more thought to multiplexing technique, dispersion management, and modulation type. Because of the signal distortion caused by dispersion, long-distance optical fibre networks may benefit from dispersion management measures. Several different kinds of long-distance optical communication systems now employ Wavelength Division Multiplexing (WDM) as a multiplexing mechanism. Advantages:

a. A higher capacity for transmission has been achieved.

b. Transmission in duplex.

c. transmission of many signals simultaneously.
d. simple system expansion.
e. New channels may be accessed quickly and at a lower cost.

3.2.2 3LCDM

Since 3LCDM allows for numerous users per channel in a WDM system, it is superior than Duty Cycle Division Multiplexing (DCDM). This article takes wavelength division multiplexing (WDM) and increases its bandwidth efficiency by mixing two data streams using a method called three-level code division multiplexing (3LCDM). Because it can quadruple capacity at a lower frequency and narrower bandwidth, 3LCDM was developed as an alternative to RZ and NRZ line coding.

Compared to the NRZ system, 3LCDM performs better in dispersion tolerance, which is a major advantage of 3LCDM. It has also come to light that the 3LCDM system, by using WDM, can support a greater number of users. However, research on 3LCDM data transmission via a WDM system is lacking.

The 3LCDM technique's encoding method is comparable to the DCDM techniques, but the 3LCDM approach's decoding procedure has its own characteristics. 3LCDM, in contrast to DCDM, which can handle more than two users on a single channel, can only manage two people. When comparing their performance with the same number of users (two users per channel), 3LCDM has a few advantages over DCDM. In contrast to the DCDM strategy, which makes use of RZ at various duty cycles, the 3LCDM system only employs RZ and NRZ line coding. DCDM is considered to have the disadvantage of requiring a guard band for the system's clock recovery because it uses more bandwidth than 3LCDM.

3.3 METHODOLOGY AND DESIGN

It is demonstrated in Figure 3.2 that the proposed two-user 3LCDM multiplexing system operates in a simulated ideal environment. Data (i.e., datal and data2) at 20 Gb/s are sent from each user through the transmitter.

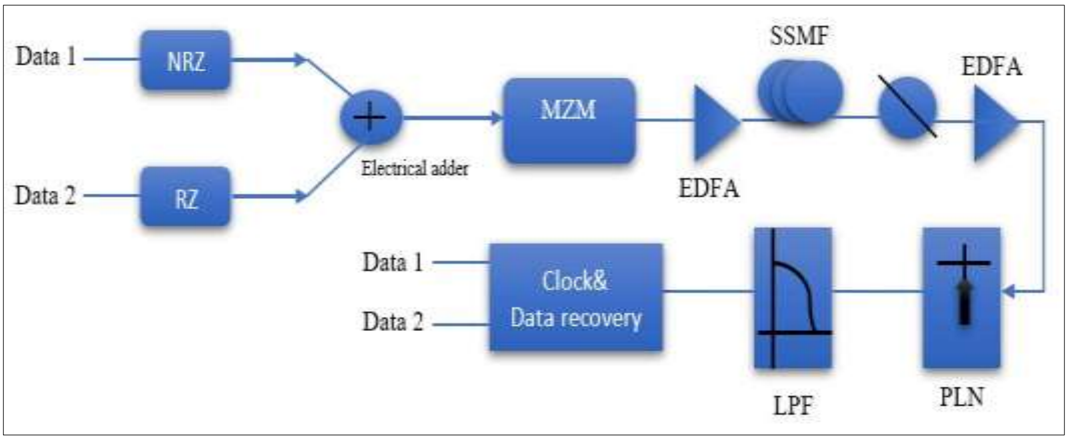

Figure 3.2: Methodology and Model.

Pressure, Year 2101. The system consists of both NRZ and RZ pulse generators. Each user's data enters a multiplexer, where it is amplified until the peak voltages are equal. The Distributed Feedback (DFB) laser operating at a line width of 10 MHz and a wavelength of 1552.5 nm will be modulated using a Mach Zehnder modulator. A low pass filter (LPF), demultiplexer, and PIN photodiode all work together to receive the optical signal. The interference is reduced by a 35 GHz cut off frequency electrical Gaussian LPF. The demultiplexer's many functions include data recovery and timing purposes. Both the clock and the data may be recovered with the use of an X-OR gate . Clock recovery is a great addition since it facilitates system deployment.

4. SIMULATIONS RESULTS

4.1 OVERVIEW

Six simulations are done at different strain levels in this chapter using the Opti system software to analyses the performance of the FBG-based sensor and the wavelength variations that follow different strain levels. In this thesis, the author uses Opti system simulation software to model the operation of a Fiber Bragg Grating installed on a power line and used as a temperature sensor. The software's GUI exhibits a transmission system to demonstrate the grating's functionality. The 25-kilometer-long fibers symbolize the distance over which a transmission is warmed by an external source, such as the sun's rays or the joule effect of energy moving through a power grid. The reflected wavelength was calculated using a model that included the spectrum of induced temperatures, the coefficient of thermal expansion, and a thermos optic coefficient. With an applied temperature gradient, a grating may selectively reflect light in a particular wavelength range by altering its period and index of refraction. When monitoring the temperature of power lines, this is the single most important output.

4.2 SIMULATIONS RESULTS

Figures 4.1 and 4.2 depict typical transmission optical signal spectra at 10Gbps for conventional NRZ over WDM and 3LCDM over WDM systems, respectively.

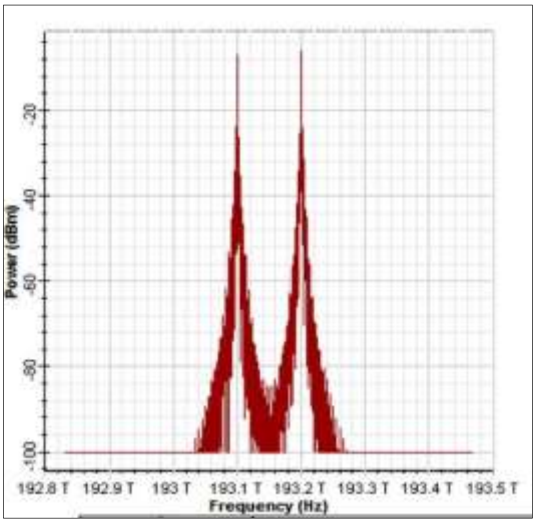

Figure 4.1: Tow Channel NRZ Over WDM.

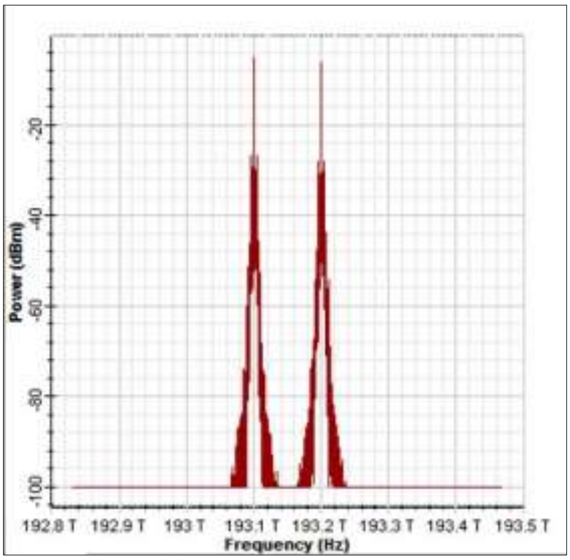

Figure 4.2: The 3LCDM over WDM System with 2 Channels.

Figures depict a typical NRZ over WDM and TLCDM over WDM system's transmitted optical signal spectra. Figure 4.3 and 4.4. According to the results of the simulations, the breadth of the optical spectrum in both the sent and received optical signals is almost the same. As can be seen in Figure 4.2, the spectrum of the transmitted optical signal is noisier when NRZ is convolved over WDM as opposed to when 3LCDM is. A 3LCDM over WDM system has a broadening impact on all four channels, as seen in Figure 4.3. (193.1 THz, 193.2 THz, 193.3 THz, and 193.4 THz). It may be inferred that 3LCDM over WDM is substantially more effective than NRZ over WDM for long-distance transmission due to the optical signal's improved noise performance.

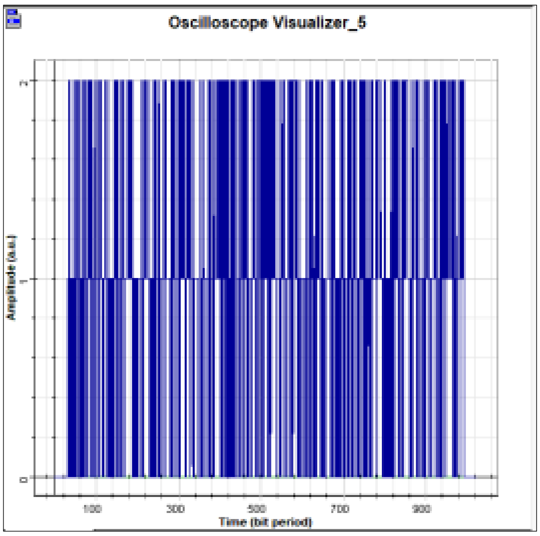

Figure 4.3: Transmitted Signal.

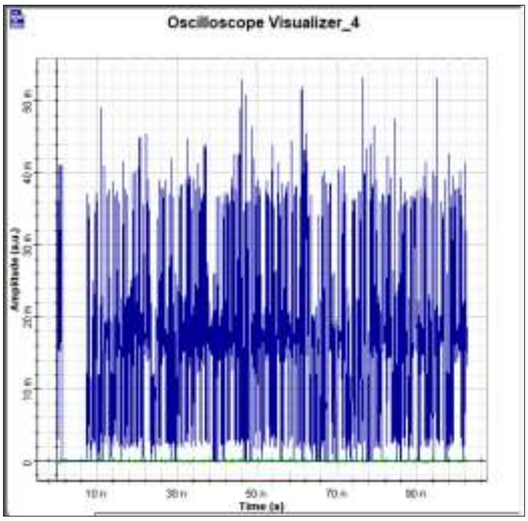

Figure 4.4: Received Signal.

Figures 4.5, display the sent and received signals, respectively, for signal and noise analysis of a 10Gbps 3LCDM over WDM system.

The transmitter broadcasts the signal at 5 Gbps by combining data from a RZ and NRZ generator. The combined signal is analysed using an oscilloscope. Figure 4.5 shows that the sent signal is free of noise, indicating that the transmitter is operating as intended. Once the signal has been processed, it is sent through optical fibre [1]. Noise is assumed to exist because of the observed fluctuations in the received signal (see Fig. 4.5). Because of losses in the optical fibre, the optical amplifier, the optical fibre, and the PIN photodetector all add to the overall noise in the system. To recover the lost signal, a PIN photodetector is used [1]. However, avalanche photodetectors (APDs) are more expensive despite their superior noise performance. One option is to use a shorter SMF.

We have modelled the effects and interactions of dispersion, attenuation, and spectral power modulation. Demonstrates this visually, the 3LCDM method may be affected by chromatic dispersion in an optical transmission system with high bit rates and long distances.

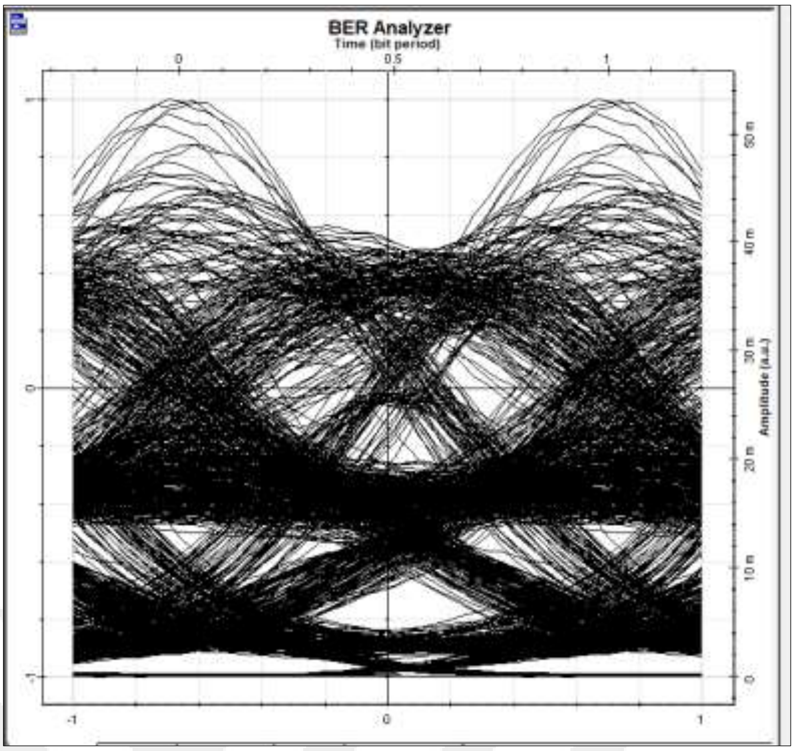

Figure 4.5: Long-Distance High-Bit-Rate Optical Transmission: Scattering's Impact on the 3LCDM Eye Diagram.

4.3 DISTANCE VS. BER

Table 4.1: Distance vs. BER of 3LCDM over WDM system.

Distance (Km)	**BER**
20	10^{-55}
40	10^{-48}
60	10^{-42}
80	10^{-33}
100	10^{-25}
120	10^{-18}
140	10^{-9}
160	10^{-5}
180	0
200	1

For a 3LCDM over WDM system running at 10 Gbps throughput, the ideal distance is shown in Table 1. Table 2 shows that for a 3LCDM over WDM system, a transmission distance of around 142 kilometers is ideal. The findings demonstrate that the dispersion control strategy used in the 3LCDM over WDM system improves the system's performance over extended distances. Long-distance transmission system performance is improved because to the incorporation of pre-DCF and two-stage EDFA into the design. The findings confirm that 3LCDM over WDM performs well enough for long-distance transmission systems.

5. CONCLUSIONS AND FUTURE WORK

5.1 CONCLUSIONS

The present writing examines a dispersion-adjusted, four-channel, 10 Gbps 3LCDM over WDM system. For the low pass, we use 40 GHz cutoff frequency Gaussian filters, and for the band pass, we use 18 GHz cutoff frequency filters. By varying the strength of the input signal, the system's optimum received power may be determined, allowing for a bit error rate (BER) of 109. For optical communications beyond 100 km, 3LCDM over WDM performs better than the standard NRZ over WDM.

5.2 FUTURE WORK

The program may be able to construct realistic signal channel counts and gain profiles automatically.

REFERENCES

[1] J. L. Kais Carranza, “Chirp-based direct phase modulation of VCSELs managed by Neural Networks.” Universitat Politècnica de Catalunya, 2019.

[2] M. Xu, Z. Jia, J. Wang, L. A. Campos, and G.-K. Chang, “Statistical data compression and differential coding for digital radio-over-fiber-based mobile fronthaul,” J. Opt. Commun. Netw., vol. 11, no. 1, pp. A60–A71, 2019.

[3] L. Shi, Vibrational Microscopy for Super-multiplexing, Vibrational Sensing and High-throughput Metabolic Imaging. Columbia University, 2020.

[4] S. Ortega, M. Halicek, H. Fabelo, G. M. Callico, and B. Fei, “Hyperspectral and multispectral imaging in digital and computational pathology: a systematic review,” Biomed. Opt. Express, vol. 11, no. 6, pp. 3195–3233, 2020.

[5] B. Morova et al., “Fabrication and characterization of large numerical aperture, high-resolution optical fiber bundles based on high-contrast pairs of soft glasses for fluorescence imaging,” Opt. Express, vol. 27, no. 7, pp. 9502–9515, 2019.

[6] B. Swiatczak, M. Feldkaemper, and F. Schaeffel, “Changes in fundus reflectivity during myopia development in chickens,” Biomed. Opt. Express, vol. 10, no. 4, pp. 1822–1840, 2019.

[7] Y. Li, P. Tang, S. Song, A. Rakymzhan, and R. K. Wang, “Electrically tunable lens integrated with optical coherence tomography angiography for cerebral blood flow imaging in deep cortical layers in mice,” Opt. Lett., vol. 44, no. 20, pp. 5037–5040, 2019.

[8] J. H. Lee et al., “Simultaneous label-free autofluorescence and multi-harmonic imaging reveals in vivo structural and metabolic changes in murine skin,” Biomed. Opt. Express, vol. 10, no. 10, pp. 5431–5444, 2019.

[9] X. He, T. Li, X. Fu, X. Jiang, Y. Gao, and X. Rao, “Fast estimation of optical properties of pear using a single snapshot technique combined with a least-squares support vector regression model based on spatial frequency domain imaging,” Appl. Opt., vol. 58, no. 15, pp. 4075–4084, 2019.

[10] M. S. Pochechuev et al., “Stain-free subcellular-resolution astrocyte imaging using third-harmonic generation,” Opt. Lett., vol. 44, no. 12, pp. 3166–3169, 2019.

[11] J.-H. Ryu, J.-H. Yang, and J. J. Yoh, “Novel utilization of the molecular band signal in metal oxides: understanding the aging process of pyrotechnic substances by using laser induced plasma emissions,” Opt. Mater. Express, vol. 9, no. 2, pp. 410–422, 2019.

[12] J. P. McLean, Y. Gan, T. H. Lye, D. Qu, H. H. Lu, and C. P. Hendon, “High-speed collagen fiber modeling and orientation quantification for optical coherence tomography imaging,” Opt. Express, vol. 27, no. 10, pp. 14457–14471, 2019.

[13] Q. He and R. K. Wang, “Analysis of skin morphological features and real-time monitoring using snapshot hyperspectral imaging,” Biomed. Opt. Express, vol. 10, no. 11, pp. 5625–5638, 2019.

[14] A. Miyazawa et al., “Polarization-sensitive optical coherence elastography,” Biomed. Opt. Express, vol. 10, no. 10, pp. 5162–5181, 2019.

[15] Z. Wu, F. Duan, J. Zhang, S. Li, H. Ma, and L. Nie, “In vivo dual-scale photoacoustic surveillance and assessment of burn healing,” Biomed. Opt. Express, vol. 10, no. 7, pp. 3425–3433, 2019.

[16] H. E. Parker et al., “Fibre-based spectral ratio endomicroscopy for contrast enhancement of bacterial imaging and pulmonary autofluorescence,” Biomed. Opt. Express, vol. 10, no. 4, pp. 1856–1869, 2019.

[17] R. Yoshimura, D.-H. Choi, M. Fujimoto, A. Uji, F. Hiwatashi, and K. Ohbayashi, “Dynamic optical coherence tomography imaging of the lacrimal passage with an extrinsic contrast agent,” Biomed. Opt. Express, vol. 10, no. 3, pp. 1482–1495, 2019.

[18] C. Guo et al., “Image-guided vibrometry system integrated with spectral-and time-domain optical coherence tomography,” Appl. Opt., vol. 58, no. 7, pp. 1606–1613, 2019.

[19] Z. Shoaib, M. A. Kamran, M. M. N. Mannan, and M. Y. Jeong, “Approach to optimize 3-dimensional brain functional activation image with high resolution: a study on functional near-infrared spectroscopy,” Biomed. Opt. Express, vol. 10, no. 9, pp. 4684–4710, 2019.

[20] X. Zhu, J.-W. Lin, and M. Y. Sander, “Infrared inhibition and waveform modulation of action potentials in the crayfish motor axon,” Biomed. Opt. Express, vol. 10, no. 12, pp. 6580–6594, 2019.

[21] J. L. Lagarto, B. T. Dyer, N. S. Peters, P. M. W. French, C. Dunsby, and A. R. Lyon, “In vivo label-free optical monitoring of structural and metabolic remodeling of myocardium following infarction,” Biomed. Opt. Express, vol. 10, no. 7, pp. 3506–3521, 2019.

[22] B. Tan et al., “Quantitative analysis of choriocapillaris in non-human primates using swept-source optical coherence tomography angiography (SS-OCTA),” Biomed. Opt. Express, vol. 10, no. 1, pp. 356–371, 2019.

[23] Y. Li, Y. Zhang, Y. Zhu, and L. Yu, “Modified biological spectrum and SNR of Laguerre-Gaussian pulsed beams with orbital angular momentum in turbulent tissue,” Opt. Express, vol. 27, no. 7, pp. 9749–9762, 2019.

[24] S. Huang et al., “Blood species identification based on deep learning analysis of Raman spectra,” Biomed. Opt. Express, vol. 10, no. 12, pp. 6129–6144, 2019.

[25] P. Rakotomanga et al., “Source separation approach for the analysis of spatially resolved multiply excited autofluorescence spectra during optical clearing of ex vivo skin,” Biomed. Opt. Express, vol. 10, no. 7, pp. 3410–3424, 2019.

[26] W. Yufeng, W. Qing, and H. Dengxin, “Preliminary exploration of atmospheric water vapor, liquid water and ice water by ultraviolet Raman lidar,” Opt. Express, vol. 27, no. 25, pp. 36311–36328, 2019.

[27] D. Borycki, M. Hamkało, M. Nowakowski, M. Szkulmowski, and M. Wojtkowski, “Spatiotemporal optical coherence (STOC) manipulation suppresses coherent cross-talk in full-field swept-source optical coherence tomography,” Biomed. Opt. Express, vol. 10, no. 4, pp. 2032–2054, 2019.

[28] D. J. Wahl, R. Ng, M. J. Ju, Y. Jian, and M. V Sarunic, “Sensorless adaptive optics multimodal en-face small animal retinal imaging,” Biomed. Opt. Express, vol. 10, no. 1, pp. 252–267, 2019.

[29] E. Zinchenko et al., “Pilot study of transcranial photobiomodulation of lymphatic clearance of beta-amyloid from the mouse brain: breakthrough strategies for non-pharmacologic therapy of Alzheimer’s disease,” Biomed. Opt. Express, vol. 10, no. 8, pp. 4003–4017, 2019.

[30] R. Turcotte, C. C. Schmidt, N. J. Emptage, and M. J. Booth, “Focusing light in biological tissue through a multimode optical fiber: refractive index matching,” Opt. Lett., vol. 44, no. 10, pp. 2386–2389, 2019.

[31] C. G. Fuentes-Corona, J. Licea-Rodriguez, R. Younger, R. Rangel-Rojo, E. O. Potma, and I. Rocha-Mendoza, “Second harmonic generation signal from type I collagen fibers grown in vitro,” Biomed. Opt. Express, vol. 10, no. 12, pp. 6449–6461, 2019.

[32] M. Z. Amin, K. K. Qureshi, and M. M. Hossain, “Doping Radius Effects on Erbium Doped Fiber Amplifier (EDFA),” 2019.

[33] K. Patorski, Ł. Służewski, P. Zdańkowski, M. Cywińska, and M. Trusiak, “Three-level transmittance 2D grating with reduced spectrum and its self-imaging,” Opt. Express, vol. 27, no. 3, pp. 1854–1868, 2019.

[34] E. Yousefi, M. Hatami, A. Torabi Jahromi, and S. Dehghani, “All-Optical Ternary Stability in Uniform Nonlinear Chalcogenide Fiber Bragg Gratings,” Int. J. Opt. Photonics, vol. 13, no. 2, pp. 103–110, 2019.

[35] M. Kues et al., “High-dimensional one-way quantum processing enabled by optical d-level cluster states,” in Quantum Information and Measurement, 2019.

[36] X. Hong, C. Fei, G. Zhang, J. Du, and S. He, “Discrete multitone transmission for underwater optical wireless communication system using probabilistic constellation shaping to approach channel capacity limit,” Opt. Lett., vol. 44, no. 3, pp. 558–561, 2019.

[37] A. Mîrzac and M. A. Macovei, “Dynamics of a quantum oscillator coupled with a three-level Λ-type emitter,” JOSA B, vol. 36, no. 9, pp. 2473–2480, 2019.

[38] S. L. Yan, “Dynamic behavior of a short cavity single-mode erbium-doped fiber laser,” in 14th National Conference on Laser Technology and Optoelectronics (LTO 2019), vol. 11170, pp. 168–174,2019.

[39] L. Stevanović, A. Maluckov, N. Filipović, and V. Pavlović, "Spatial solitary like weak probe wave in the three-level Λ-type atoms," in AIP Conference Proceedings, vol. 2075, no. 1,2019.

[40] W. C. Wang, B. Zhou, S. H. Xu, Z. M. Yang, and Q. Y. Zhang, "Recent advances in soft optical glass fiber and fiber lasers," Prog. Mater. Sci., vol. 101, pp. 90–171, 2019.

[41] T. Matniyaz et al., "Diffraction-limited Yb-doped double-clad all-solid photonic bandgap fiber laser at 976 nm," in Fiber Lasers XVI: Technology and Systems, vol. 10897, pp. 146–151,2019.

[42] S. J. Whiteley et al., "Spin–phonon interactions in silicon carbide addressed by Gaussian acoustics," Nat. Phys., vol. 15, no. 5, pp. 490–495, 2019.

[43] H.-H. Huang, E. Li, and H. Wang, "Three-level equilibrium strategy of DC voltage balance control for H-bridge cascaded active power filter," IEEE Access, vol. 7, pp. 28847–28854, 2019.

[44] A. N. A. J. Abbood and H. S. Al-Raweshidy, "Digital fronthaul link based on optimised digital radio over fibre system," Iet Optoelectron., vol. 13, no. 6, pp. 259–266, 2019.

[45] X. Li, C. Min, S. Gao, G. Sun, X. Chen, and H. Chen, "A CDMA-based high-speed multi-access VLC system with OOK modulation," Opt. Commun., vol. 451, pp. 147–152, 2019.

[46] V. Tikhonov, V. Berezovsky, and J. Nvoba, "THE PERSPECTIVES OF SATELITE COMMUNICATION DEVELOPMENT," ОРГКОМІТЕТ КОНФЕРЕНЦІЇ, pp. 73, 2019.

[47] P. Roztocki et al., "Kerr combs and telecommunications components for the generation and high-dimensional quantum processing of d-level cluster states," in 2019 21st International Conference on Transparent Optical Networks (ICTON), pp. 1–3,2019.

[48] W. Chen, J. Gu, Q. Li, X. Tang, and D. Chen, "Geometrically invariant watermarking for medical images based on digital holography and three-level DWT-SVD," Appl. Opt., vol. 58, no. 15, pp. 4185–4191, 2019.

[49] C. Reimer et al., “High-dimensional one-way quantum computation operations with on-chip optical d-level cluster states,” in CLEO: QELS_Fundamental Science, pp. FTh1A-4,2019.

[50] T. Matniyaz et al., “Highly efficient cladding-pumped single-mode three-level Yb all-solid photonic bandgap fiber lasers,” Opt. Lett., vol.44, pp. 807–810, 2019.

[51] X. Liu et al., “Energy-time entanglement-based dispersive optics quantum key distribution over optical fibers of 20 km,” Appl. Phys. Lett., vol. 114, no. 14, pp. 141104, 2019.

[52] O. P. Swami, V. Kumar, B. Suthar, and A. K. Nagar, “A theoretical study of the propagation of light soliton produced by semiconductor quantum dots through optical fibers,” Наносистемы: физика, химия, математика, vol. 10, no. 3, pp. 273–281, 2019.

[53] O. P. Swami, V. Kumar, B. Suthar, and A. K. Nagar, “A theoretical study of light soliton produced by semiconductor quantum dot waveguides and propagation in optical fibers,” Вестник Московского государственного технического университета им. НЭ Баумана. Серия «Естественные науки», pp. 89–102, 2019.

[54] N. Borgohain and S. Konar, “Broadband mid-infrared supercontinuum generation in three-level multiple quantum wells using short optical pulses,” Opt. Laser Technol., vol. 120, pp. 105684, 2019.

[55] M. Ghasemi and M. K. Tavassoly, “Quantum repeater using three-level atomic states in the presence of dissipation: stability of entanglement,” J. Phys. B At. Mol. Opt. Phys., vol. 52, no. 8, pp. 85502, 2019.

[56] R. Ahmad, W. Ko, K. S. Feder, and P. S. Westbrook, “Measuring the shape of microbends in optical fibers,” Opt. Lett., vol. 45, no. 18, pp. 5189–5192, 2020.

[57] S. Girard et al., “Recent advances on radiation-hardened optical fiber technologies,” in Optical Fiber Communication Conference,pp. W1C-3,2020.

[58] O. Kotlyar, M. Pankratova, M. Kamalian-Kopae, A. Vasylchenkova, J. E. Prilepsky, and S. K. Turitsyn, “Combining nonlinear Fourier transform and neural network-based processing in optical communications,” Opt. Lett., vol. 45, no. 13, pp. 3462–3465, 2020.

[59] J. Lian and M. Brandt-Pearce, "Multiuser visible light communication systems using OFDMA," J. Light. Technol., vol. 38, no. 21, pp. 6015–6023, 2020.

[60] L. Rosa, S. H. Pallangal, F. Poli, S. Selleri, and A. Cucinotta, "Mode phase variation and sensitivity to thermal load in three-core optical fibers," J. Light. Technol., vol. 38, no. 8, pp. 2400–2405, 2020.

[61] Y. Wen et al., "Compact and high-performance vortex mode sorter for multi-dimensional multiplexed fiber communication systems," Optica, vol. 7, no. 3, pp. 254–262, 2020.

[62] J. Shi, N. Sun, and Z. Xia, "Invulnerability Analysis of Electric Power Optical Transmission Network in Smart Grid Based on Complex Networks," in Journal of Physics: Conference Series,2020.

[63] M. J. Barber, P. C. Shardlow, P. Barua, J. K. Sahu, and W. A. Clarkson, "Nested-ring doping for highly efficient 1907 nm short-wavelength cladding-pumped thulium fiber lasers," Opt. Lett., vol. 45, no. 19, pp. 5542–5545, 2020.

[64] M. Hohn et al., "Energy-time entanglement from a resonantly driven quantum dot three-level system," arXiv Prepr. arXiv2301.05697, 2023.

[65] T. Hao, "Research of Optical Interconnection Technology in Datacenter Networks," in Journal of Physics: Conference Series, vol.1710, no.1, pp.12001.2020.

[66] C. P. Reddy, R. Ramaraghavulu, T. Kalpana, and J. Gajendiran, "Energy transfer induced enhancement in NIR luminescence characteristics of Yb3+/Er3+ co-doped sodium zinc bismuth fluorophosphate glasses," Opt. Mater. (Amst)., vol. 100, pp. 109616, 2020.

[67] M. Dai, H. Liu, and L. Wei, "Explicit solutions of coupled-mode equations for multiple waveguide devices: The optical analogy of a three-state geometric phase," Optik (Stuttg)., vol. 201, pp. 163329, 2020.

[68] S. H. I. Zhipeng, W. Huinan, W. Chanqiong, W. Xiaodong, W. Jinming, and L. I. Shijie, "Research on UPIoT application of low-voltage station area based on dual-mode communication," in 2020 12th IEEE PES Asia-Pacific Power and Energy Engineering Conference (APPEEC), pp. 1–6,2020.

[69] Z. He and F. Hu, “Research on novel modulation format Apol-FSK for optical transport network of 5G,” Opt. Commun., vol. 474, pp. 126055, 2020.

[70] J. Shi et al., “User-specific power level allocation optimization for OFDM-NOMA in a multi-user RoF system,” Opt. Lett., vol. 45, no. 16, pp. 4436–4439, 2020.

[71] M. Yoshida, N. Takefushi, K. Kasai, T. Hirooka, and M. Nakazawa, “Precise measurements and their analysis of GAWBS-induced depolarization noise in various optical fibers for digital coherent transmission,” Opt. Express, vol. 28, no. 23, pp. 34422–34433, 2020.

[72] D. Zhang, D. Liu, X. Wu, and D. Nesset, “Progress of ITU-T higher speed passive optical network (50G-PON) standardization,” J. Opt. Commun. Netw., vol. 12, no. 10, pp. D99–D108, 2020.

[73] N. A. Naser, M. R. Harb, and H. A. Yasser, “Analytical Model of Pulse Amplification in Erbium Doped Fiber Amplifier,” MJPS, vol. 7, no. 2, 2020.

[74] I. M. Mirza, J. G. Hoskins, and J. C. Schotland, “Dimer chains in waveguide quantum electrodynamics,” Opt. Commun., vol. 463, pp. 125427, 2020.

[75] D. B. Talam, E.-S. A. El-Badawy, H. M. H. Shalaby, and M. H. Aly, “EDFA gain flattening using fiber Bragg gratings employing different host materials,” Opt. Quantum Electron., vol. 52, pp. 1–17, 2020.

[76] M. Singh, D. Kumar, and D. Somwanshi, “Design and Analysis of Ultra High Speed 16 Channel Cascaded EDF A-DWDM Network with Post Dispersion Compensations Using Optimization of Fiber Bragg Grating,” in 2020 5th IEEE International Conference on Recent Advances and Innovations in Engineering (ICRAIE), 2020.

[77] G. Vanderhaegen et al., “Observation of doubly periodic solutions of the nonlinear Schrödinger equation in optical fibers,” Opt. Lett., vol. 45, no. 13, pp. 3757–3760, 2020.

[78] K. S. Rajasree, T. Ray, K. Karlsson, J. L. Everett, and S. N. Chormaic, “Generation of cold Rydberg atoms at submicron distances from an optical nanofiber,” Phys. Rev. Res., vol. 2, no. 1, pp. 12038, 2020.

[79] L. Costa et al., “Fast and direct measurement of the linear birefringence profile in standard single-mode optical fibers,” Opt. Lett., vol. 45, no. 3, pp. 623–626, 2020.

[80] S. Gao, “Automatic detection and monitoring system of pantograph–catenary in China’s high-speed railways,” IEEE Trans. Instrum. Meas., vol. 70, pp.1–12, 2020.

[81] S. S. Aleshkina et al., “High-order mode suppression in double-clad optical fibers by adding absorbing inclusions,” Sci. Rep., vol.10, no. 1, pp. 7174, 2020.

[82] R. M. Ibrahim, “Effect of Temperature on the Gain Characteristics of Erbium Doped Optical Fiber Amplifiers.”

[83] V. H. Nguyen, I. Bugar, M. Longobucco, R. Buczyński, B. A. Malomed, and M. Trippenbach, “Reversible ultrafast soliton switching in dual-core highly nonlinear optical fibers,” Opt. Lett., vol. 45, no.18, pp. 5221–5224, 2020.

[84] H. Nouri and M. Uysal, “Experimental investigation on the effect of wavelength on aperture averaging in FSO communications,” Opt. Lett., vol.45, no.11, pp. 3063–3066, 2020.

[85] H. Yokohashi, S. Matsukawa, M. Sato, Y. Toba, S. Kurokawa, and H. Murata, “Antenna-coupled-electrode electro-optic modulator for converting two orthogonal-polarization field components simultaneously for 5G mobile systems,” in Conference on Lasers and Electro-Optics/Pacific Rim, p. C8F_3,2020.

[86] N. Takefushi, M. Yoshida, K. Kasai, T. Hirooka, and M. Nakazawa, “Theoretical and experimental analyses of GAWBS phase noise in various optical fibers for digital coherent transmission,” Opt. Express, vol. 28, no. 3, pp. 2873–2883, 2020.

[87] M. Pan, X. Wen, Y. Chen, Z. Lu, Z. Wang, and L. Wang, “A Cloud Radio Access Network Simulation Platform for Networked Automatic Driving,” in 2020 IEEE 6th International Conference on Computer and Communications (ICCC), pp. 839–845,2020.

[88] M. Irfan et al., “DSP-Assisted nonlinear impairments tolerant 100 Gbps optical backhaul network for long-haul transmission,” Entropy, vol.22, no.9, pp.1062, 2020.